Atmos. Chem. Phys. Discuss., 11, 32583–32600, 2011
www.atmos-chem-phys-discuss.net/11/32583/2011/
doi:10.5194/acpd-11-32583-2011


Atmospheric Chemistry and Physics Discussions



# $CO_2(\nu_2)$-O quenching rate coefficient derived from coincidental SABER/TIMED and Fort Collins lidar observations of the mesosphere and lower thermosphere

**A. G. Feofilov**[1], **A. A. Kutepov**[2,3], **C.-Y. She**[4], **A. K. Smith**[5], **W. D. Pesnell**[3], **and R. A. Goldberg**[3]

[1]Centre National de la Recherche Scientifique/École Polytechnique, UMR8539, Palaiseau-Cedex, 91128, France
[2]The Catholic University of America, Washington DC, 20064, USA
[3]NASA Goddard Space Flight Center, Greenbelt, MD, 20771, USA
[4]Colorado State University, Fort Collins, CO, 80523, USA
[5]National Center for Atmospheric Research, Boulder, 80307, CO, USA

Received: 24 October 2011 – Accepted: 1 December 2011 – Published: 9 December 2011

Correspondence to: A. G. Feofilov (artem.feofilov@lmd.polytechnique.fr)

Published by Copernicus Publications on behalf of the European Geosciences Union.

## Abstract

Among the processes governing the energy balance in the mesosphere and lower thermosphere (MLT), the quenching of $CO_2(\nu_2)$ vibrational levels by collisions with O atoms plays an important role. However, there is a factor of 3–4 discrepancy between various measurements of the $CO_2$-O quenching rate coefficient, $k_{VT}$. We retrieve $k_{VT}$ in the altitude region 80–110 km from coincident SABER/TIMED and Fort Collins sodium lidar observations by minimizing the difference between measured and simulated broadband limb 15 µm radiances. The retrieved $k_{VT}$ varies from about $5 \times 10^{-12}$ cm$^3$ s$^{-1}$ at 87 km to about $7 \times 10^{-12}$ cm$^3$ s$^{-1}$ at 104 km. A detailed consideration of retrieval errors and uncertainties indicates deficiency in current understanding the non-LTE formation mechanism of atmospheric 15 µm radiances. An updated mechanism of $CO_2$-O collisional interactions is suggested.

## 1 Introduction

Infrared emission in 15 µm $CO_2$ band ($I_{15\,\mu m}$) is the dominant cooling mechanism in the Earth's mesosphere and lower thermosphere (MLT) (Gordiets et al., 1976; Dickinson, 1984; Goody and Yung, 1989; Sharma and Wintersteiner, 1990). On Earth, the magnitude of MLT cooling affects both the mesopause temperature and height; the stronger the cooling, the colder and higher is the mesopause (Bougher et al., 1994). The $I_{15\,\mu m}$ radiance is also used to retrieve vertical temperature distributions ($T[z]$) in Earth's atmosphere by a number of satellite instruments: CRISTA (Offermann et al., 1999), SABER (Russell et al., 1999), MIPAS (Fischer et al., 2008). The main mechanisms linking the 15 µm $CO_2$ atmospheric radiation to the heat reservoir (translational degrees of freedom atmospheric constituents) are the inelastic collisions of $CO_2$ molecules with $O(^3P)$ atoms: first, atomic O excites the $CO_2$ bending vibrational mode during the collision:

$$CO_2(\nu_2) + O(^3P) \leftrightarrow CO_2(\nu_2+1) + O(^3P) \quad (1)$$

after which the excitation may be quenched either by other collision with some molecule or atom or by emission of the radiation quantum: $CO_2(v_2+1) \rightarrow CO_2(v_2) + h\nu$ (667 $cm^{-1}$), where $v_2$ is the bending mode quantum number. Both the cooling efficiency and $I_{15\,\mu m}$ strongly depend on the rate coefficient of process (1) and on the atomic O volume mixing ratio (VMR). To be consistent with a generally accepted way of describing this process we will refer to the rate coefficient of the reaction inverse to (1) and will call it the "$CO_2$-O quenching rate coefficient" or $k_{VT}$, where VT index stands for vibrational-translational type of interaction. Generally, it is assumed that the velocity distribution of atomic oxygen is Maxwellian, and that the fine structure of atomic oxygen does not affect the process (1) and its inverse. First we will use these assumptions that are typical for atmospheric modeling and then will address their applicability in the discussion part of the work (Sect. 4).

It is self-evident that both the calculation of radiative cooling/heating rates in $CO_2$ and the interpretation of measured $I_{15\,\mu m}$ radiances require the best possible knowledge of $k_{VT}$. However, despite the importance of $k_{VT}$ for the atmospheric applications, the values, obtained in laboratory or retrieved by fitting the space observations, vary by a factor of *3–4* (see Table 1 and Sect. 3 below for more details). In this work we describe the retrieving of $k_{VT}$ from coincidental space and lidar observations. For this purpose we used the extensive dataset provided by the SABER instrument (Russell et al., 1999) aboard TIMED satellite that contains, besides other information, vertical profiles of $I_{15\,\mu m}(z)$, O($z$), and, more recently, $CO_2(z)$ (Rezac, 2011) VMRs. This dataset was supplemented with $T(z)$ in 80–110 km altitude range measured by Fort Collins lidar (40.6° N,105.2° W). We show that the synergy of these two instruments enables one to retrieve $k_{VT}$ and study its behavior in the MLT. All calculations presented in this work were carried out using the non-LTE ALI-ARMS code package (Kutepov et al., 1998; Gusev and Kutepov, 2003). The background for the non-LTE problem for the molecular gas and the review of $k_{VT}$ measurements and estimates is given in the next section.

## 2 Non-LTE problem for the molecular gas in atmosphere and $k_{VT}$ rate coefficient

Inelastic molecular collisions determine the population of molecular levels in the lower atmosphere. As a result local thermodynamic equilibrium (LTE) exists where the populations obey the Boltzmann law with the local kinetic temperature. In the MLT the frequency of collisions is lower and the vibrational levels populations must be found taking into account all processes which populate and depopulate vibrational levels: optical transitions, chemical sources, vibrational-vibrational and vibrational-translational energy exchange processes, and the absorption of atmospheric and solar radiation in the ro-vibrational bands. The altitude above which the LTE approximation is not applicable depends on the relationship between these processes and for $CO_2(\nu_2)$ vibrational levels involved in forming of $I_{15\,\mu m}$ the non-LTE effects become important above ~ 75–80 km altitude (López-Puertas and Taylor, 2001; Kutepov et al., 2006).

The importance of $k_{VT}$ rate coefficient for the calculation of $CO_2$ emission in MLT was first discussed by Crutzen (1970). He suggested an estimate for this value with the upper limit of $3.0 \times 10^{-13}\,cm^3\,s^{-1}$. First laboratory measurement of $k_{VT}$ were performed at high temperatures ($T > 2000$ K) (Center, 1973) using shock tube technique. The extrapolations of these measurements to room temperatures by fitting the Landau-Teller expression (Taylor, 1974) provided values of $2.4 \times 10^{-14}\,cm^3\,s^{-1}$. The average value of this rate coefficient obtained in later studies has changed by two orders of magnitude and since the middle of 1980-s the $k_{VT}$ is accepted to be on the order of $(1.0–10.0) \times 10^{-12}\,cm^3\,s^{-1}$ (see the overview of $k_{VT}$ measurements and estimates in Table 1). However, as we show below these variations are still large both for the adequate estimation of the radiative budget of MLT region and for temperature retrievals from 15 µm $CO_2$ radiance. There is a well known discrepancy between the laboratory measurements of $k_{VT}$ and its retrieval from the atmospheric measurements. Generally, laboratory measurements provide low values of $k_{VT}$ centered around $1.3 \times 10^{-12}\,cm^3\,s^{-1}$. Huestis et al. (2008) based on the analysis of experimental data and quantum mechanical calculations recommends using $k_{VT} = 1.5 \times 10^{-12}\,cm^3\,s^{-1}$. However, using this



ACPD
11, 32583–32600, 2011

value leads to overestimating MLT temperatures from 15 µm radiance measurements and the values required for an adequate interpreting of atmospheric measurements are usually about $5.5 \times 10^{-12}\,\mathrm{cm^3\,s^{-1}}$ with the exception of $k_{VT} = 1.5 \times 10^{-12}\,\mathrm{cm^3\,s^{-1}}$ retrieved by Vollmann and Grossmann (1997) from the sounding rocket observations.

To demonstrate the influence of $k_{VT}$ on the MLT area we performed a sensitivity study for an average midlatitude atmospheric profile using a standard set of V-V and V-T rate coefficients (Kutepov et al., 2006) and $k_{VT}$ that was first set to $1.5 \times 10^{-12}\,\mathrm{cm^3\,s^{-1}}$ and then to $6.0 \times 10^{-12}\,\mathrm{cm^3\,s^{-1}}$. The results are presented in Fig. 1a–c. Figure 1a demonstrates the population of the first $\nu_2$-excited level shown as vibrational temperature (see the figure caption for the vibrational temperature definition). After obtaining the non-LTE populations of all vibrational levels involved in the task the broadband $I_{15\,\mu m}$ (Fig. 1b) was simulated in line by line mode and the resulting spectrum was convolved with the "narrow" 15 µm SABER bandpass function. The total cooling/heating rate is shown in Fig. 1c. As one can see the MLT area is sensitive to the $k_{VT}$ changes above ∼85 km altitude. Below this level the sensitivity rapidly decreases and 80 km altitude can be considered as a "threshold" between LTE and non-LTE for $CO_2(\nu_2)$ levels and the lower limit for the $k_{VT}$ retrieval. The upper limit is defined by the fading of the signal strength with increasing altitude.

## 3 Retrieving $k_{VT}$ from the overlapping SABER and lidar measurements

### 3.1 The $k_{VT}$ retrieval approach

The general idea for the $k_{VT}$ rate coefficient retrieval from overlapping satellite and lidar measurements is in minimizing the difference between the measured and simulated 15 µm radiance by varying the $k_{VT}$. The simulations are performed with the "reference" temperature profiles measured by the lidar instrument and, therefore, not affected by uncertainties the $k_{VT}$. A similar approach was utilized by Feofilov et al. (2009) who used the $H_2O$ VMR profiles measured by ACE-FTS instrument as reference ones and estimated three rate coefficients important for the calculation of $H_2O(\nu_2)$ populations in MLT. Retrieving the $k_{VT}$ from comparing the measured and simulated 15 µm radiances is somewhat more complicated because the $CO_2(\nu_2)$ populations depend not only on $k_{VT}$ but also on atomic oxygen concentration (or VMR) that contributes to uncertainties in retrieved $k_{VT}$. The way of overcoming this limitation will be described below. First, let us consider the simplified case of a single overlap for which everything excluding $k_{VT}$ is known. Since calculations demonstrate monotonic dependence of $CO_2(\nu_2)$ populations and limb radiances on $k_{VT}$ at all altitudes (see Fig. 1a,b in this work and Sect. 3.6.5.1 in López-Puertas and Taylor, 2001), the deviation $\zeta(k_{VT},z) = |I_{meas}(z) - I_{simul}(k_{VT},z)|$ will have a single minimum at each altitude z and in the ideal case of noiseless signal the retrieved rate coefficient will be unique. Adding the noise to the experimental radiance $I_{meas}(z)$ and uncertainties to calculated radiance $I_{simul}(k_{VT},z)$ that are linked with uncertainties in lidar temperatures and spatiotemporal variability of the area will blur the minimum of $\zeta$ $(k_{VT},z)$ that will, finally, define the uncertainty for the $k_{VT}$ retrieval. Let us now consider the case when both atomic oxygen concentration [O] and $k_{VT}$ are not known. This exercise is important since even though SABER retrieves individual $[O](z)$ profiles (Mlynczak et al., 2007), any offsets or errors in $[O](z)$ (Smith et al., 2010) will propagate to $k_{VT}$. However, this problem might be overcome if the average $[O]_{aver}(z)$ profile is known with a sufficient accuracy (from climatology, modeling or other measurements). In this case one can search for a minimum of $\zeta(\gamma,z)$ with respect to a new variable $\gamma = k_{VT} \times [O]$ over a large number of SABER/lidar overlaps. At this stage individual uncertainties of $[O](z)$ do not play any role. Important is to choose a grid on $\gamma$ in such a way that the following criteria are satisfied: a) $\gamma$ variation range includes the $\gamma_{min}$ value that corresponds to absolute minimum of $\zeta$ $(z,\gamma)$; b) the grid step is fine enough to hit the minimum of $\zeta$ $(z,\gamma)$. When the minimum of $\zeta$ $(z,\gamma)$ is found over a large number of overlaps, one can retrieve the optimal value of rate coefficient: $k_{VT} = \gamma_{min} / [O]_{aver}$ for each altitude point where $[O]_{aver}$ is the average value of atomic oxygen concentration obtained either from SABER or from other sources. At this point the accuracy of $[O]_{aver}(z)$ becomes important that will be discussed below.

## 3.2 Using the Colorado State Sodium lidar temperature measurements for $k_{VT}$ retrievals

In this study we used $I_{15\,\mu m}(z)$, $T(z)$, $P(z)$, $CO_2(z)$, and $O(z)$ from SABER V1.07 database and coincidental $T(z)$ measured by the Colorado State Sodium lidar described in details in (She et al., 2003). Briefly, the lidar is a two-beam system capable of simultaneous measurement of mesopause region temperature and winds, day and night, weather permitting. This lidar has been modified in 1999 in response to TIMED satellite objectives. The lidar setup can perform simultaneous measuring of mesopause region Na density, temperature, zonal and meridional wind profiles with both daytime and nighttime capability. The measurement precision of the lidar system for temperature and wind with 2 km spatial resolution and 1 h integration time were estimated for each beam under nighttime fair sky conditions to be, respectively, 0.5 K and 1.5 m s$^{-1}$ at the Na peak (92 km), and 5 K and 15 m s$^{-1}$ at the edges (81 and 107 km) of the Na layer. Depending on the purpose of the analysis, the temporal resolution may be made between 10 min and several hours. We have searched for SABER/lidar simultaneous common volume measurements in 2002–2005 using stringent criteria for time and space overlapping: $\Delta\text{lat} < 2^\circ$, $\Delta\text{long} < 2^\circ$, $\Delta t < 10$ min. Most of the profiles selected in this way (85%) fall in 18–6 h local time interval. We substituted SABER $T(z)$ in 80–110 km altitude range with the corresponding lidar $T(z)$ and hydrostatically adjusted $P(z)$ to new $T(z)$. Atomic O is changing in this period and using individual $O(z)$ is not reasonable, therefore we used the $\gamma = k_{VT} \times O$ variable discussed in Sect. 3.1. To reduce the number of runs with obviously incorrect $\gamma$ values, we used the following approach: at each altitude the grid on $\gamma$ was built using the available $O(z)$ and 21 points for $k_{VT}$ in the $(1.0–10) \times 10^{-12}$ cm$^3$ s$^{-1}$ range with $5 \times 10^{-13}$ cm$^3$ s$^{-1}$ step. The correctness of the $\gamma$ grid selection was verified at each altitude and for each overlapping event by checking for the existence of the $\zeta(\gamma, z)$ minimum. For each overlapping event the non-LTE populations of $CO_2$ vibrational levels were found at all altitudes and $I_{15\,\mu m}$ was simulated in line by line mode and then convolved with the corresponding SABER bandpass function. This procedure was repeated for all grid points of the $\gamma$ variable. Then at each altitude point z we calculated the radiance difference $\zeta(\gamma,z)$ (Fig. 2a). As one can see all $\zeta(\gamma,z)$ curves up to 105 km (cyan curve) have a clear minimum $\zeta_{min}(\gamma,z)$ that washes out for $\zeta(\gamma,z)$ dependencies above that altitude. This behavior is explained both by larger lidar $T(z)$ and by larger $I_{15\,\mu m}(z)$ uncertainties at higher altitudes. The values of $\gamma$ corresponding to $\zeta_{min}(\gamma,z)$ form a separate scientific product $\gamma_{min}(z)$ that may be used in midlatitude atmospheric applications for cooling/heating rate and $I_{15\,\mu m}$ calculations. The retrieved $\gamma_{min}(z)$ values are $7.4\times10^{-16}$; $1.0\times10^{-14}$; $5.3\times10^{-14}$; $1.9\times10^{-13}$; $5.2\times10^{-13}$; $6.4\times10^{-13}$; $9.8\times10^{-13}$ [$cm^3\,s^{-1}$] for $z = 80$; 85; 90; 95; 100; 105; 110 km, respectively. To obtain the $k_{VT}(z)$ profile (Fig. 2c) we divided the $\gamma_{min}(z)$ profile by average atomic O VMR profile, $O_{aver}(z)$, (Fig. 2b). The error bars in Fig. 2c represent standard deviations estimated from input data uncertainties.

## 4 Discussion

Overall, the $k_{VT}(z)$ values shown in Fig. 2b fit well to the atmospheric retrievals: the averaged value of $k_{VT}$ is equal to $6.1\pm1.7\times10^{-12}\,cm^3\,s^{-1}$. However, Fig. 2c also demonstrates the altitudinal variability of $k_{VT}(z)$ that goes beyond its uncertainties in 85–105 km altitude range. Obviously, this variability does not imply that $k_{VT}$ rate coefficient depends on altitude. Let us consider possible reasons for the observed $k_{VT}$ behavior. The retrieved $k_{VT}(z)$ depends on: a) lidar $T(z)$ in 80–110 km, b) SABER $P(z)$ and $T(z)$ below 80 km, c) $I_{15\,\mu m}(z)$ d) $CO_2(z)$, e) $O(z)$, f) $CO_2$ non-LTE model. Offsets in any of these parameters will lead to offsets in the retrieved $k_{VT}(z)$. One can exclude a)-d) since their uncertainties have been included in the analysis. The most important component for $k_{VT}(z)$ retrieval is $O_{aver}(z)$. A detailed analysis of SABER V1.07 data shows that the O density is at least twice that from other data sources (Smith et al., 2010 and references therein). However, reducing $O_{aver}(z)$ by factor of two will mean increasing $k_{VT}(z)$ by the same factor, which will make it 8–10 times larger than the laboratory measured values. On the other hand, further increasing $O_{aver}(z)$ to compensate for the $k_{VT}(z)$ increase with altitude cannot be justified using the current model of $O(z)$ production in MLT (Smith et al., 2010). The $T(z)$ uncertainties used in $O(z)$ retrieval in SABER V1.07 can not lead to significant changes in $O_{aver}(z)$, either. The remaining possibility is the simplicity of the $CO_2$ non-LTE model with respect to $CO_2$-O collisions. The standard pumping term in the non-LTE model, which describes total production of $CO_2(\nu_2)$ in the state with the number of bending mode quanta $\nu_2$ due to collisions with the $O(^3P)$ atoms has the form of

$$Y_{\nu_2} = n_{O(^3P)}\{n_{\nu_2-1}k_{\nu_2-1,\nu_2} - n_{\nu_2}k_{\nu_2,\nu_2-1}\} \tag{2}$$

where $n_{O(^3P)}$ is the $O(^3P)$ density, $n_{\nu_2-1}$ and $n_{\nu_2}$ are the vibrational states populations, and $k_{\nu_2-1,\nu_2}$ and $k_{\nu_2,\nu_2-1}$ are rate coefficients for one-quantum excitation and de-excitation, respectively. In current non-LTE models, including the one applied in this study, it is usually assumed that $k_{\nu_2-1,\nu_2} = k_{0,1}$ and $k_{\nu_2,\nu_2-1} = k_{1,0}$. It follows from Huestis et al. (2008) that if the velocity distribution of $O(^3P)$ atoms is Maxwellian and their fine stricture is thermalized then the laboratory measured $k_{0,1}$ and $k_{1,0}$ are linked by the detailed balance relation:

$$k_{0,1} = k_{1,0}\cdot\frac{g_1}{g_0}\cdot e^{-E_1/(kT)} \tag{3}$$

where $g_0$ and $g_1$ are the statistical weights of the lower and upper vibrational states, respectively, $E_1$ is the vibrational energy of the first $\nu_2$ vibrational level, $k$ is the Boltzmann constant, and $T$ is the local kinetic temperature. Sharma et al. (1994) showed that both above mentioned conditions are valid for $O(^3P)$ atoms in the Earth's atmosphere up to at least 400 km, which seems justifying usage of Eqs. (2) and (3) in the non-LTE models. However, as Balakrishnan et al. (1998) and Kharchenko et al. (2005) show, the non-thermal $O(^3P)$ and $O(^1D)$ atoms are produced by $O_2$ and $O_3$ photolysis and $O_2^+$ dissociative recombination reactions in the MLT. These "hot" atoms may serve as an additional source of $CO_2(\nu_2)$ level excitation. Therefore, the expression Eq. (2)





ACPD
11, 32583–32600, 2011

may need to be replaced by the expression like

$$Y_{\nu_2} = n_{O(^3P)} \cdot \left[ (\alpha - 1) \cdot \left\{ n_{\nu_2-1} k_{\nu_2-1,\nu_2} - n_{\nu_2} k_{\nu_2,\nu_2-1} \right\} + \alpha \cdot \left\{ \sum_{\nu} n_{\nu_2-\nu} k^{\text{hot}}_{\nu_2-\nu,\nu_2} - n_{\nu_2} \sum_{\nu} k^{\text{hot}}_{\nu_2,\nu_2-\nu} \right\} \right] \quad (4)$$

where $\alpha$ is the fraction of total $O(^3P)$ density which corresponds to hot atoms, $k^{\text{hot}}_{\nu_2-\nu,\nu_2}$ and $k^{\text{hot}}_{\nu_2,\nu_2-\nu}$ are the rate coefficients for excitation and de-excitation of $CO_2$ molecules, respectively, due to collisions with hot atoms, assuming also multi-quantum processes. These rate coefficients are not related by the detailed balance since hot $O(^3P)$ are not thermalized. Comparing Eq. (2) which is applied in the model used in our study with Eq. (4), one can see that the rate coefficient values retrieved in this work and in other atmospheric studies are some sort of effective rate coefficient which may be expressed as

$$k^{\text{retr}}_{1,0}(z) = k^{\text{retr}}_{\nu_2,\nu_2-1}(z) = (\alpha(z) - 1) \cdot k_{\nu_2-1,\nu_2} + \alpha(z) \cdot \sum_{\nu} n_{\nu_2} k^{\text{hot}}_{\nu_2-\nu,\nu_2} \quad (5)$$

that includes the contribution of hot $O(^3P)$ atoms. The simplistic analysis given above is not intended to explain our result. It, however, may indicate the direction toward its interpretation. We obviously see $k^{\text{retr}}_{1,0}(z)$ increasing with altitude. This may reflect the increasing contribution of hot $O(^3P)$ atoms whose concentration is increasing with altitude.

## 5 Summary

We have presented a methodology for retrieving values of $k_{VT}$ and $\gamma = k_{VT} \times O$ (where O is the VMR of atomic oxygen) from atmospheric observations and applied it to overlapping SABER and Fort Collins lidar measurements. The obtained $\gamma$ values are





ACPD
11, 32583–32600, 2011

$7.4 \times 10^{-16}$; $1.0 \times 10^{-14}$; $5.3 \times 10^{-14}$; $1.9 \times 10^{-13}$; $5.2 \times 10^{-13}$; $6.4 \times 10^{-13}$; $9.8 \times 10^{-13}$ [$cm^3\,s^{-1}$] at 80; 85; 90; 95; 100; 105; 110 km, respectively. The average value of the retrieved $k_{VT}$ in 80–110 km altitude range is $6.1 \pm 1.7 \times 10^{-12}\,cm^3\,s^{-1}$. We also observed an altitude dependence of the retrieved $k_{VT}$ that varies from $4.9 \pm 0.3 \times 10^{-12}\,cm^3\,s^{-1}$ at 87 km to $7.2 \pm 0.3 \times 10^{-12}\,cm^3\,s^{-1}$ at 104 km. The observed variation may be linked to a simplification in the traditional consideration of $CO_2(\nu_2) + O(^3P)$ interactions. We show that both the altitude variation of "atmospheric" $k_{VT}$ and its discrepancy from the laboratory measurements may be explained by subdividing the oxygen atoms to "normal" and "excited" or "hot" groups, with the different $k_{VT}$ rate coefficients for each of the groups. Comparisons with other lidar locations as well as quantum mechanical calculations for the collisions of $CO_2$ with "hot" O atoms are needed to further study the observed phenomenon. Depending on the mechanism that will be revealed in the course of these additional studies, the radiative cooling rate calculations for general circulation models should be performed in accordance with the fractionizing defined by Eq. (4). For the temperature retrievals from the 15 µm $CO_2$ atmospheric radiance observations we recommend using $k_{1,0}^{retr}(z)$ values obtained in this work.

*Acknowledgements.* This research was partially supported under NASA grant NNX08AG41G. NCAR is sponsored by the National Science Foundation. The authors would like to thank Peter Wintersteiner and Richard Picard for their comments on the preliminary version of the manuscript and David Huestis for the discussion regarding the detailed balance in $CO_2(\nu_2) + O(^3P)$ collisions.

cnrs INSU
Institut national des sciences de l'Univers

The publication of this article is financed by CNRS-INSU.

## References

Allen, D., Scragg, C. T., and Simpson, C. J. S. M.: Low temperature fluorescence studies of the deactivation of the bend-stretch manifold of $CO_2$, Chem. Phys., 51, 279–298, 1980.

Balakrishnan, N., Kharchenko, V., and Dalgarno, A.: Slowing of energetic $O(^3P)$ atoms in collisions with $N_2$, J. Geophys. Res., 103, 23,393–23,398, 1998.

Bougher, S. W., Hunten, D. M., and Roble, R. G.: $CO_2$ cooling in terrestrial planet thermospheres, J. Geophys. Res., 99, 14609–14622, 1994.

Castle, K. J., Kleissas, K. M., Rhinehart, J. M., Hwang, E. S., and Dodd, J. A.: Vibrational relaxation of $CO_2(\nu_2)$ by atomic oxygen, J. Geophys. Res., 111, A09303, doi:10.1029/2006JA011736, 2006.

Center, R. E.: Vibrational relaxation of $CO_2$ by O atoms, J. Chem. Phys., 59(7), 3523–3528, 1973.

Crutzen, P. J.: Discussion of paper "Absorption and emission by carbon dioxide in the atmosphere" by Houghton, J. T., Q. J. Roy. Metor. Soc., 96, 767–770, 1970.

Dickinson, R. E.: Infrared radiative cooling in the mesosphere and lower thermosphere, J. Atmos. Sol. Terr. Phys., 46, 995–1008, 1984.

Feofilov, A. G., Kutepov, A. A., Pesnell, W. D., Goldberg, R. A., Marshall, B. T., Gordley, L. L., García-Comas, M., López-Puertas, M., Manuilova, R. O., Yankovsky, V. A., Petelina, S. V., and Russell III, J. M.: Daytime SABER/TIMED observations of water vapor in the mesosphere: retrieval approach and first results, Atmos. Chem. Phys., 9, 8139–8158, doi:10.5194/acp-9-8139-2009, 2009.

Fischer, H., Birk, M., Blom, C., Carli, B., Carlotti, M., von Clarmann, T., Delbouille, L., Dudhia, A., Ehhalt, D., Endemann, M., Flaud, J. M., Gessner, R., Kleinert, A., Koopman, R., Langen, J., López-Puertas, M., Mosner, P., Nett, H., Oelhaf, H., Perron, G., Remedios, J., Ridolfi, M., Stiller, G., and Zander, R.: MIPAS: an instrument for atmospheric and climate research, Atmos. Chem. Phys., 8, 2151–2188, doi:10.5194/acp-8-2151-2008, 2008.

Goody, R. M. and Yung, Y. L.: Atmospheric Radiation, Oxford Univ. Press, New York, NY, 1989.

Gordiets, B. F.: A model of the upper atmosphere radiating in infrared spectrum, Kratkie Soobsh. Fiz., 6, 40, 1976.

Gordiets, B. F., Kulikov, Y. U. N., Markov, M. N., and Marov, M. Ya.: Numerical modelling of the thermospheric heat budget, J. Geophys. Res., 87(A6), 4504–4514, 1982.

Gusev, O. A. and Kutepov, A. A.: Non-LTE gas in planetary atmospheres, in: Stellar Atmosphere Modeling, ASP Conference Series, 288, edited by: Hubeny, I., Mihalas, D., and Werner, K., 318–330, Stellar Atmosphere Modeling, Tuebingen, Germany, 8–12 April, 2002, 2003.

Gusev, O., Kaufmann, M., Grossmann K. U., Schmidlin, F. J., and Shepherd, M. G.: Atmospheric neutral temperature distribution at the mesopause/turbopause altitude, J. Atmos. Sol. Terr. Phys., 68, 1684–1697, doi:10.1016/j.jastp.2005.12.010, 2006.

Huestis, D. L., Bougher, S. W., Fox J. L., Galand, M., Johnson, R. E., Moses J. I., and Pickering, J. C.: Cross sections and reaction rates for comparative planetary aeronomy, Space Sci. Rev., 139, 63–105, doi:10.1007/s11214-008-9383-7, 2008.

Kharchenko, V., Dalgarno, A., and Fox, J. L.: Thermospheric distribution of fast $O(^1D)$ atoms, J. Geophys. Res., 110, A12305, doi:10.1029/2005JA011232, 2005.

Khvorostovskaya, L. E., Potekhin, I. Yu., Shved, G. M., Ogibalov V. P., and Uzyukova, T. V.: Measurement of the rate constant for quenching $CO_2(01^10)$ by atomic oxygen at low temperatures: reassessment of the rate of cooling by the $CO_2$ 15-µm Emission in the Lower Thermosphere, Izvestiya Atmos. Ocean. Phys., 38, 613–624, 2002.

Kumer, J. B. and James, T. C.: SPIRE data evaluation and nuclear IR fluorescence processes, Report DNAOOI-79-C-0033, AFGL, Bedford, Mass., 1983.

Kutepov, A. A., Gusev, O. A., and Ogibalov, V. P.: Solution of the non-LTE problem for molecular gas in planetary atmospheres: superiority of accelerated lambda iteration, J. Quant. Spectrosc. Radiat. Transf. 60, 199, 1998.

Kutepov, A. A., Feofilov, A. G., Marshall, B. T., Gordley, L. L., Pesnell, W. D., Goldberg, R. A., and Russell III, J. M.: SABER temperature observations in the summer polar mesosphere and lower thermosphere: Importance of accounting for the $CO_2$ $\nu_2$ quanta V–V exchange, Geophys. Res. Lett., 33, L21809, doi:10.1029/2006GL026591, 2006.

Lilenfeld, H. V.: Deactivation of Vibrationally-Excited NO and $CO_2$ by O-Atoms, Final technical rept., 28 September 1989–15 Jun 1994, available at: http://handle.dtic.mil/100.2/ADA298581, last access: 8 Dec 2011, ADA298581, 1994.

López-Puertas, M. and Taylor, F. W.: Non-LTE Radiative Transfer in the Atmosphere, Singapore: World Scientific, 2001.

Mlynczak, M. G., Marshall, B. T., Martin-Torres, F. J., Russell III, J. M., Thompson, R. E., Remsberg, E. E., and Gordley, L. L.: Sounding of the atmosphere using broadband emission radiometry observations of daytime mesospheric $O_2(^1\Delta)$ 1.27 µm emission and derivation of ozone, atomic oxygen, and solar and chemical energy deposition rates, J. Geophys. Res.,

112(D15306), doi:10.1029/2006JD008355, 2007.
Mlynczak, M. G., Martin-Torres, F. J., Johnson, D. G., Kratz, D. P., Traub, W. A., and Jucks, K.: Observations of the $O(^3P)$ fine structure line at 63 µm in the upper mesosphere and lower thermosphere, J. Geophys. Res., 109, A12306, doi:10.1029/2004JA010595, 2004.
Offermann, D., Grossmann, K. U., Barthol, P., Knieling, P., Riese, M, and Trant, R.: Cryogenic Infrared Spectrometers and Telescopes for the Atmosphere (CRISTA) experiment and middle atmosphere variability, J. Geophys. Res., 104, 16311–16325, doi:10.1029/1998JD100047, 1999.
Pollock, D. S., Scott, G. B. I., and Phillips, L. F.: Rate constant for quenching of $CO_2$(010) by atomic oxygen, Geophys. Res. Lett., 20, 727–729, 1993.
Ratkowski, A. J., Picard, R. H., Winick, J. R., Grossmann, K. U., Homann, D., Ulwick, T. J. C., and Paboojian, A. J.: Lower-thermospheric infrared emissions from minor species during high-latitude twilight-B. Analysis of 15 µm emission and comparison with non-LTE models, J. Atmos. Terr. Phys., 56, 1899–1914, 1994.
Rezac, L.: Simultaneous retrieval of $T(p)$ and $CO_2$ volume mixing ratio from limb observations of infrared radiance under non-LTE conditions, Ph.D. thesis, Hampton University of Virginia, 163 pp., 2011.
Russell III, J. M., Mlynczak, M. G., Gordley, L. L., Tansock, J. J., and Esplin, R.: Overview of the SABER experiment and preliminary calibration results, P. Soc. Photo.-Opt. Ins., 3756, 277–288, 1999.
Sharma, R. D.: Infrared airglow, in: Progress in Atmospheric Physics: Proceedings of the 15th Annual Meeting on Atmospheric Studies by Optical Methods, edited by: Rodrigo, R., López-Moreno, J. J., López-Puertas, M., Molina, A., Kluwer Academic Publishers, Boston, 177–186, 1987.
Sharma, R. D. and Nadile, R. M.: Carbon dioxide ($\upsilon_2$) radiative results using a new non-equilibrium model, AIAA-81-0426, AIAA 19th Aerospace Sciences Meeting, St. Louis, 12–15 Jan 1981, 1981.
Sharma, R. D. and Wintersteiner, P. P.: Role of carbon dioxide in cooling planetary thermospheres, Geophys. Res. Lett., 17, 2201–2204, 1990.
Sharma, R., Zygelman, B., von Esse, F., and Dalgarno, A.: On the relationship between the population of the fine structure levels of the ground electronic state of atomic oxygen and the translational temperature, Geophys. Res. Lett., 21, 1731–1734, 1994.
She, C.-Y., Sherman, Y. J., Yuan, T., Williams, B. P., Arnold, K., Kawahara, T. D., Li, T., Xu, L.





ACPD
11, 32583–32600, 2011

$CO_{2(\nu_2)}$-O quenching rate coefficient

A. G. Feofilov et al.

Title Page
Abstract | Introduction
Conclusions | References
Tables | Figures
◂ ▸
Back | Close
Full Screen / Esc
Printer-friendly Version
Interactive Discussion

F., Vance, J. D., Acott, P., and Krueger, D. A.: The first 80-h continuous lidar campaign for simultaneous observation of mesopause region temperature and wind, Geophys. Res. Lett., 30, 1319–1323, doi:10.1029/2002GL016412, 2003.

Shved, G. M., Khvorostovskaya, L. E., Potekhin, I. Yu., Demyanikov, A. I., Kutepov, A. A., and Fomichev, V. I.: Measurement of the quenching rate constant for collisions $CO_2$ $(01^10)$–O: the importance of the rate constant magnitude for the thermal regime and radiation of the lower thermosphere, Izv. Atmos. Ocean. Phys., 27, 431–437, 1991.

Smith, A. K., Marsh, D. R., Mlynczak, M. G., and Mast, J. C.: Temporal variations of atomic oxygen in the upper mesosphere from SABER, J. Geophys. Res., 115, D18309, doi:10.1029/2009JD013434, 2010.

Stair, A. T., Jr., Sharma, R. D., Nadile, R. M., Baker, D. J., and Grieder, W. F.: Observations of limb radiance with cryogenic spectral infrared rocket experiment, J. Geophys. Res., 90(A10), 9763–9775, 1985.

Taylor, R.: Energy transfer processes in the stratosphere, Can. J. Chem., 52, 1436–1451, 1974.

Vollmann, K. and Grossmann, K. U.: Excitation of 4.3 µm $CO_2$ emissions by $O(^1D)$ during twilight, Adv. Space Res., 20(6), 1185–1189, 1997.





ACPD
11, 32583–32600, 2011

**Table 1.** Historical review of $k_{VT}\{CO_2\text{-}O\}$ quenching rate coefficient measurements and atmospheric retrievals at $T = 300$ K.

| $k_{VT}\{CO_2\text{-}O\}$ [$cm^3 s^{-1}$] | Reference | Comments |
|---|---|---|
| $3–30 \times 10^{-14}$ | Crutzen (1970) | First guess |
| $2.4 \times 10^{-14}$ | Taylor (1974), Center (1973) | Laboratory measurements |
| $5.0 \times 10^{-13}$ | Sharma and Nadille (1981) | Atmospheric retrieval |
| $1.0 \times 10^{-12}$ | Gordiets et al. (1982) | Numerical experiment |
| $2.0 \times 10^{-13}$ | Kumer and James (1983) | Atmospheric retrieval |
| $2.0 \times 10^{-13}$ | Dickinson (1984); Allen (1980) | Laboratory measurements |
| $5.2 \times 10^{-12}$ | Stair et al. (1985) | Atmospheric retrieval |
| $3.5 \times 10^{-12}$ | Sharma, (1987) | Atmospheric retrieval |
| $3–9 \times 10^{-12}$ | Sharma and Wintersteiner (1990) | Atmospheric retrieval |
| $1.5 \times 10^{-12}$ | Shved et al. (1991) | Laboratory measurements |
| $1.3 \times 10^{-12}$ | Pollock et al. (1993) | Laboratory measurements |
| $5.0 \times 10^{-12}$ | Ratkowski et al. (1994) | Atmospheric retrieval |
| $5.0 \times 10^{-13}$ | Lilenfeld (1994) | Laboratory measurements |
| $1.5 \times 10^{-12}$ | Vollmann and Grossmann (1997) | Atmospheric retrieval |
| $1.4 \times 10^{-12}$ | Khvorostovskaya et al. (2002) | Laboratory measurements |
| $1.8 \times 10^{-12}$ | Castle et al. (2006) | Laboratory measurements |
| $6.0 \times 10^{-12}$ | Gusev et al. (2006) | Atmospheric retrieval |
| $1.5 \times 10^{-12}$ | Huestis et al. (2008) | Recommended value |

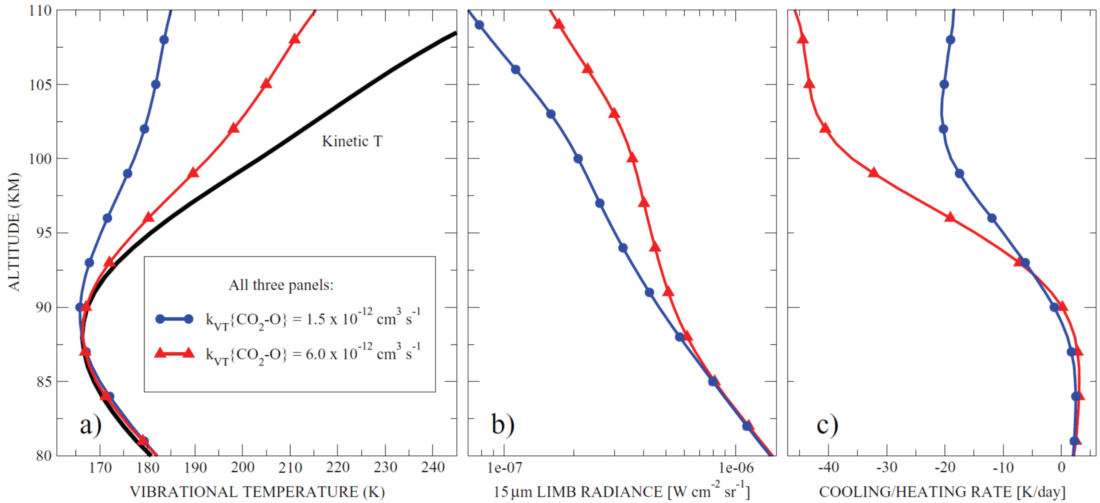


**Fig. 1.** The sensitivity of **(a)** $CO_2(010)$ main isotope vibrational level populations, **(b)** $I_{15\,\mu m}(z)$, and **(c)** infrared cooling/heating rate in $CO_2$ bands to $k_{VT}$. Lines with circles: $k_{VT} = 1.5 \times 10^{-12}\,\mathrm{cm^3\,s^{-1}}$; lines with triangles: $k_{VT} = 6.0 \times 10^{-12}\,\mathrm{cm^3\,s^{-1}}$. The non-LTE populations in panel **(a)** are presented as vibrational temperatures that define the vibrational level excitation against the ground level 0: $n_1/n_0 = g_1/g_0 \exp[-(E_1 - E_0)/kT_v]$, where $n_{0,1}$, $g_{0,1}$, and $E_{0,1}$ are populations, degenerations, and energies of the ground state and first vibrational level, respectively.





ACPD

11, 32583–32600, 2011

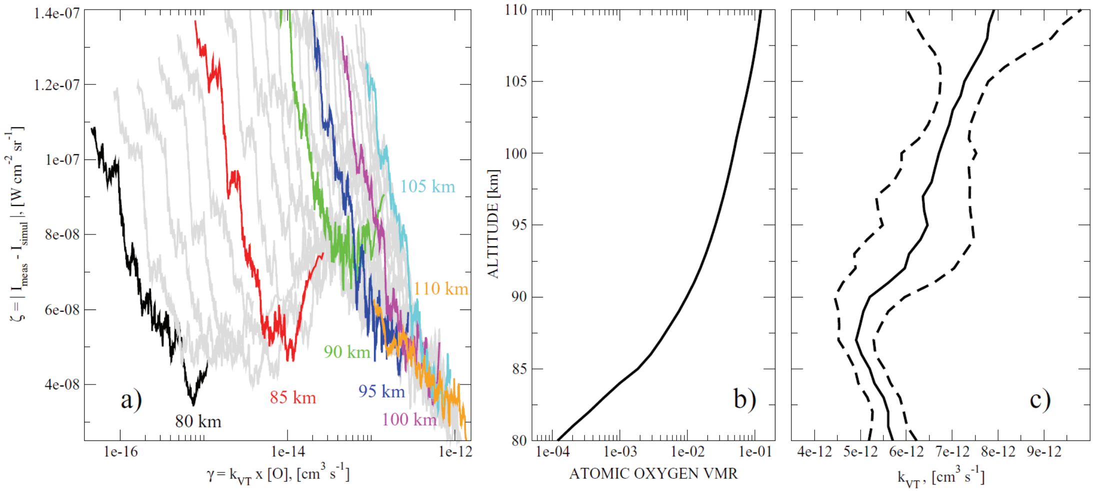


**Fig. 2.** Estimating the optimal $k_{VT}$ from overlapping SABER and lidar measurements: **(a)** deviations between calculated and measured $I_{15\,\mu m}$ at different altitudes with respect to a combined $\gamma$ value (see text). Each $\zeta(\gamma,z)$ curve in this panel represents the average over 72 individual deviations. Note the existence of $\zeta(\gamma,z)$ minima at all heights up to 105 km (cyan curve) that washes out above this altitude (e.g. no minima for orange curve); **(b)** average [O]($z$) built for all overlapping events; **(c)** solid line: $k_{VT}(z)$ obtained as a result of dividing the individual minima found in the left panel by atomic O VMRs from the middle panel; dashed lines: standard deviations for $k_{VT}$.